JOURNAL OF CATALYSIS 126, 326–338 (1990)

Kinetics and Characterization of Bismuth Molybdate Catalysts

II. Reaction Studies over Various Bimolybdates

P. M. BURBAN,*,[1] G. C. A. SCHUIT,* T. A. KOCH,*,† AND K. B. BISCHOFF*

*Department of Chemical Engineering, Center for Catalytic Science and Technology, University of Delaware, Newark, Delaware 19716; and †Du Pont Experimental Station, Petrochemicals Department, Wilmington, Delaware 19898

Received April 16, 1990; revised July 19, 1990

The model reaction, 1-butene to 1,3-butadiene, was studied over various compositions of unsupported bismuth molybdates to rank the catalysts' reactivities. Following Matsuura *et al.* we confirmed that γ-Bi_2MoO_6 doped with bismuth to yield a surface Bi/Mo > 2.0 is unselective; selective catalyst species need a few mole% excess MoO_3. All catalysts with a surface Bi/Mo ≤ 1.5 show selectivities to butadiene greater than 95%. As the amount of MoO_3 increases, reducing the surface Bi/Mo ratio, the activity increases down to Bi/Mo = 1.5, then remains constant down to Bi/Mo = 1, and then decreases steadily down to Bi/Mo = $\frac{2}{3}$. Characteristics of the partial oxidation catalysis change drastically going from γ-Bi_2MoO_6 to α-Bi_2MoO_{12} catalysts. For the model reaction, Bi_2MoO_6 + 4% MoO_3 exhibits an E_a = 40 kJ/mol (9.5 kcal/mol) at temperatures above 673 K. This catalyst is completely poisoned by its product butadiene below 673 K, while the inhibition is lifted above this temperature. We suggest that the pores of this catalyst, estimated to be 24 nm in diameter, become filled with "polybutadiene"; the heat of butadiene adsorption was estimated to be 375 kJ/mol. In contrast, α-$Bi_2Mo_3O_{12}$ is not inhibited by butadiene, and has a lower activity (even calculated per unit surface) with an activation energy of 93 kJ/mol over the entire temperature range 660–713 K, studied. We propose models which describe two distinct ensemble effects operative in determining the kinetics over selective γ-Bi_2MoO_6 and α-$Bi_2Mo_3O_{12}$ catalysts.

INTRODUCTION

Over the past 20 years, numerous papers have been published about the selective oxidation of olefins over bismuth molybdate catalysts (*1–4*). The main features of the proposed catalytic cycles are recapitulated here to set the stage for findings reported in this paper. By about 1970, several hypotheses were generally accepted for the mechanism of selective oxidation of olefins over bismuth molybdates. For the two reactions, propylene to acrolein and 1-butene to 1,3-butadiene, the first elementary step, assumed rate determining, consisted of the dissociation of a H atom from the α carbon atom next to the double bond, thereby forming an allylic intermediate on the catalysts' surface (*5*). The oxygen atoms responsible for partial oxidation were delivered from the catalyst according to the Mars–Van Krevelen catalytic cycle (*6*). The reduced catalyst was rapidly reoxidized by dissociative adsorption of gas phase oxygen on the same adsorption site used by the olefin. The reaction was therefore claimed (*7, 8*) to be independent of oxygen partial pressure in the temperature range 600 to 773 K and to be inhibited by the products below 650 K.

Partial oxidation of propene and butene over bismuth molybdates is very selective provided the Bi/Mo bulk ratios remain in the range $\frac{2}{3}$ < Bi/Mo < $\frac{2}{1}$. Bi_2O_3 and MoO_3 are catalytically active only above 725 K, with the former being unselective and the latter moderately selective. In the active

[1] Author to whom correspondence should be addressed. Current address: University of Minnesota–Duluth, Department of Chemical Engineering, 10 University Drive, 231 Engineering Bldg., Duluth, MN 55812-2496.

0021-9517/90 $3.00

range, three compounds are known to exist: γ-Bi_2MoO_6 (Koechlinite), α-$Bi_2Mo_3O_{12}$, and β-$Bi_2Mo_2O_9$ (thermodynamically stable only between 823 and 1023 K) (*9–11*). Bi_2MoO_6 is converted to another structure (γ') above 873 K. Maximum activity is usually reported at a bulk Bi/Mo about one; the pure α phase is reported to be only weakly active and opinions differ considerably as to the activity of the γ phase. According to Batist *et al.* (*12*), the pure γ phase is very active while Matsuura *et al.* (*13*) maintained that it is inactive but becomes very active when doped with 2–4% MoO_3.

In the course of time, it became apparent that the reaction mechanisms were more complicated than originally presumed. Matsuura *et al.* (*14–16*) reported measurements on the adsorption of 1-butene and propene which they found, in both cases, to be dissociative but already fast and weak below 350 K with an enthalpy of adsorption of 50 kJ/mol. Butadiene showed two types of adsorption, one weak and fast with similar adsorption enthalpy to the olefins but also another that was activated, associative, and with an adsorption enthalpy of 84 kJ/mol. These observations indicated that the first reaction step, the dissociation of H, was not necessarily rate determining.

Even more interesting were the tracer oxygen-18 experiments performed by Keulks and Krenzke (*17, 18*). Their results showed that the oxidation of the olefin could take place at a site different from that where reoxidation of the reduced catalyst occurred. For some catalysts such as Bi_2MoO_6, the site where protons are donated to the catalyst is situated at a different surface plane than that where oxygen enters the partially reduced catalyst. During the reaction the catalyst is a semiconductor, as shown by Van Oeffelen *et al.* (*19*), and oxygen migration through the bulk may be rate determining.

There are than two major points of controversy. One concerns the question of which elementary reaction(s) is (are) actually rate determining. The other is whether there are two sites with different functions specifically connected with different cations and, if so, on which site hydrocarbon oxidation and catalyst reoxidation occur, respectively? A most attractive theory is that of Burrington and Grasselli (*21–23*): the first reaction should be the dissociation of a proton to a surface oxygen connected with Bi^{3+} while the residual allylic species becomes bonded via σ–π bonding to a neighboring Mo^{6+} cation that subsequently becomes reduced. Via electron transport through the solid, electrons are then transferred to Bi and from there to O_2. The rate determining reaction then might be electron or anion transport through the lattice. Bi has two functions and the first step occurs on a Bi/Mo pair. Haber *et al.* (*24*) postulate that the first step takes place only on bismuth.

The experiments to be represented in this paper were conducted because the authors had come to the opinion that the kinetics of the butene dehydrogenation over Bi-molybdates were not well understood. There were several effects that cased this lack of knowledge. One had to do with the exothermicity of the reaction that might have resulted in serious temperature gradients ("hotspots") in the microreactors so often applied. Another cause of discrepancies found their origin in analytical uncertainties as to the surface Bi/Mo ratios. Difficulties arising from both these error sources will form the subject of the present paper. Still another problem is given by the fact that active site densities as determined by Matsuura *et al.* (*14–16*) for Bi molybdate catalysts were performed at much lower temperatures and hence their relevance is open to some doubt. The present paper is particularly concerned with the analytical problems and the high-temperature kinetics.

EXPERIMENTAL

Catalyst preparation, the laboratory fixed bed reactor system, and the on-line analysis of reaction products were discussed in the first paper (*25*), Part I, where it was shown that the laboratory fixed bed reactor was

operated in near gradientless fashion. Details of experimental methods can be found elsewhere (*26*).

Several hundred grams of both Bi_2MoO_6 and $Bi_2Mo_3O_{12}$ were prepared (see (*25*)) and random samples were found to have reproducible activities and selectivities at identical feed conditions. Using this standard composition of catalyst, the compositions of these "base case" catalysts were altered by impregnation using the "incipient wetness" method. Approximately 0.15 to 0.45 ml of impregnating solution was used per gram of catalyst, depending on the catalyst surface area and desired overall composition. A standard gravimetric technique was used (*26*) to determine the molybdenum content in representative samples of all compositions of bismuth molybdates synthesized. A typical standard deviation of ±0.1% was obtained for all Bi_2MoO_6 catalysts containing an average of 22.3% molybdenum.

X-ray photoelectron spectroscopy (XPS) was used to quantify the relative surface compositions of the various catalysts. An ESCA/Auger system equipped with a Mg anode X-Ray source ($K\alpha$ line of −1235.6 eV) was operated using an ESCA Multiplex routine. A list of all catalysts prepared, their code numbers, particle sizes, surface areas, and bulk and surface Bi/Mo values are given in Table 1. Recapitulating from Part I (*25*), selectivity was defined as a percentage of the ratio of butene conversion to butadiene divided by the total butene conversion to diene plus carbon dioxide. In the next section, results are divided into two groups. The first group contains the results of preliminary experiments to facilitate a comparison with findings of earlier workers. In the second group, results of exploratory experiments on the kinetics of butene are presented.

TABLE 1

Listing of All Bi Molybdate Catalysts' Compositions, Surface Areas and Particle Sizes (from (*26*))

Catalyst origin	Code no.	S.A. m^2/g	d_p μm	Bi/Mo atomic ratio	
				Bulk	Surface (XPS)
Bi_2MoO_6	Base Case; A		550	1.87	
Bi_2MoO_6	Base Case; A1	3.4	550		
Bi_2MoO_6	Base Case; A2		550		
Bi_2MoO_6	Base Case; A3		320		1.7
Bi_2MoO_6	Base Case; A3	2.5	>45		1.6
Bi_2MoO_6	Base Case; A5		550		1.8
A + 4.0% Mo	A7	3.1	390	1.81	1.4, 1.4, 1.5
A + 4.0% Mo	A8	2.5	550		
A + 2.0% Mo	A10		550	1.90	1.4
A + 6.2% Bi	A11	2.8	390	1.91	1.6, 1.6, 1.6
A + 9.4% Bi	A12	2.7	550	1.92	2.2, 2.2, 2.1
A12 + 5% Mo	AN23	2.6	550	1.83	1.6
A + 4.0% Mo	A36	2.7	320	1.81	1.3, 1.4
A + 4.0% Mo	A37	2.5	320	1.81	1.5
$Bi_2Mo_3O_{12}$	Base Case; B		320	0.58	0.4
$Bi_2Mo_3O_{12}$	Base Case; B1		320	0.61	
$Bi_2Mo_3O_{12}$	Base Case; B2		320	0.60	0.4
$Bi_2Mo_3O_{12}$	Base Case; B3		320	0.61	0.6
$Bi_2Mo_3O_{12}$	Base Case; B4	0.72	320	0.61	0.6
B + 6.6% Bi	B8	0.74	320		0.3, 0.3

RESULTS

Preliminary Studies

All catalysts with a surface Bi/Mo ≤ 1.5 showed selectivities to butadiene greater than 95%, with blank corrected selectivities typically approaching 100%. Since it was difficult to uncouple the background combustion blank reactions from CO_2 formation over bismuth molybdates, no further quantitative analysis was done. One catalyst, Bi_2MoO_6 + 9.4% Bi (surface Bi/Mo = 2.2), was an exception to the exclusively high selectivities: its selectivities were 73% at 680 K and 83% at 713 K at activities half those found for base case Bi_2MoO_6 catalysts compared at identical conditions. Figure 1 illustrates the change of surface Bi/Mo values as a function of bulk Bi/Mo values, the latter in the range between 0.5 and 2.2. A similar plot was earlier published by Matsuura *et al.* (*13*) and the two data sets agree very well; it is seen that the surface Bi/Mo values of the stoichiometric compounds are near those of the bulk. However, in the bulk range between 1 and 1.8 the surface composition remains equal to 1, as found by both groups, whereas the bulk phase X-ray diffraction patterns show a mixture of α and γ (*26*). Evidently, the metastable β phase

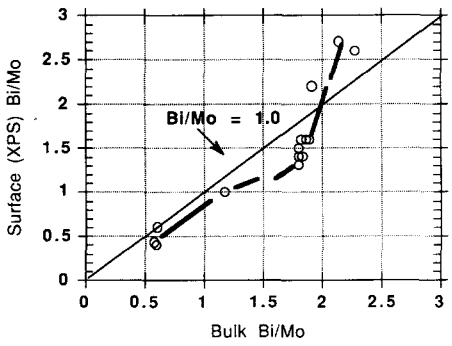

FIG. 1. Surface (XPS) versus bulk (elemental analysis) Bi/Mo ratios for various Bi molybdate catalysts synthesized by precipitation and impregnation.

dissociates into α and γ but the surface retains the Bi/Mo = 1 composition.

Figure 2 presents our differential butadiene production rates (for analysis, see (*25*)) in gmol/(m^2sec) as a function of the Bi/Mo surface ratio at 659 and 704 K. Again, there is agreement with Matsuura's data but now agreement is only qualitative; our conversions at equal temperatures are considerably lower, as shown in Table 2, which is attributable to "hotspots" present in Matsuura *et al.*'s near adiabatic microreactor, especially at 713 K (*27*). The semiquantitative agreement is, however, satisfactory in many ways; we both find that Bi_2MoO_6 doped with bismuth to yield a surface Bi/Mo > 2.0 is unselective and less active, contrary to Batist's assumption. The discrepancy can be explained by the steep fall of rate when the bulk and surface Bi/Mo value approach 2 and by past analytical uncertainties in determining Mo concentrations in catalysts (*27*). The next point concerns the butadiene inhibition. Figure 3 shows the conversion of 1-butene over Bi_2MoO_6 + 5% MoO_3 as a

TABLE 2

Comparison of Catalyst Performance: (1) This Work, Sample A11; (2) Sample "M", from Matsuura *et al.* (*13*)

Catalyst	Bi/Mo atomic ratio		S.A. m^2/g	Total S.A. m^2
	Bulk	Surface (XPS)		
A11	1.6	1.9	2.8	1.12[a]
"M"	1.53	1.92	3.2	1.00
Catalyst	Conversion to butadiene (%)		Selectivity to butadiene (%)	
	673 K	713 K	673 K	713 K
A11	22	36	95	99
"M"	40	62	"greater than 95%"	

[a] The catalyst bed contained 0.4 g of catalyst A11 and 1.4 g SiC diluent. Sample "M" was run in the catalyst bed undiluted.

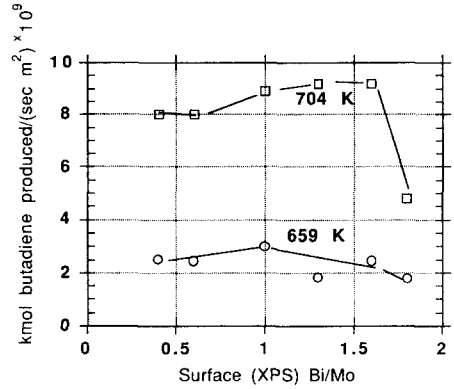

FIG. 2. Differential rate of butadiene formation over various bismuth molybdate catalysts with varying surface composition at constant feed conditions: 10.3 C_4H_8: 14.7 O_2: 75 He; F_T = 995 sccm, and W = 0.4 g catalyst.

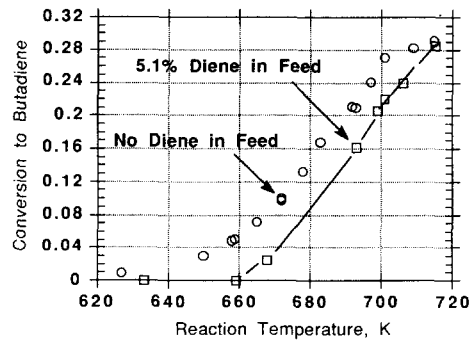

FIG. 3. Effect of butadiene inhibition over Bi_2MoO_6 at constant feed conditions: 10% C_4H_8, 10% O_2, 80% He, F_T = 596 sccm, and W = 0.4 g catalyst.

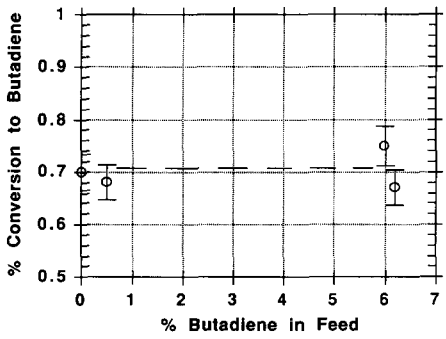

FIG. 4. Effect of butadiene inhibition over $Bi_2Mo_3O_{12}$ at 659 K and constant feed conditions: 10.3% C_4H_8, 14.7% O_2, F_T = 995 sccm, and W = 0.4 g catalyst.

function of temperature for a side-by-side comparison: (i) a feed mixture with partial pressure ratios of 1 C_4H_8 : 1 O_2 : 8 He and (ii) an identical feed mixture, except that 5 (vol)% of the original total He flow was replaced with butadiene. It is clear that the partial oxidation rate with the latter feed was considerably slower than in the original feed mixture free of butadiene. In contrast, for similar experiments for feed with and without butadiene, no inhibition occurred over base case $Bi_2Mo_3O_{12}$ catalysts, as shown in Fig. 4.

Exploratory Kinetic Studies

Figure 5 and Table 3 display results of experiments conducted to determine

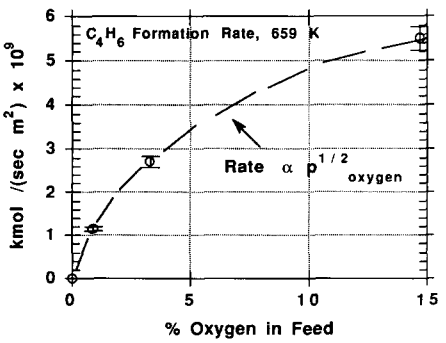

FIG. 5. Effect of oxygen partial pressure on the differential rate of butadiene formation over 0.4 g Bi_2MoO_6 at constant feed conditions: 10.3% C_4H_8, F_T = 995 sccm.

TABLE 3

Dependence of Oxygen Partial Pressure on the Differential Rate of Butadiene over Bi_2MoO_6 and $Bi_2Mo_3O_{12}$ for a Fixed Total Pressure, Flowrate, F_T, and Butene Composition (Oxygen Compositions 14.7, 3.3, and 1.0%)

	T (K)	n
	Bi_2MoO_6	
A31-3	659	0.51
A36	659	0.51
A38	659	0.50
A36	659	0.51
A31-3	704	0.14
A38	704	0.18
	$Bi_2Mo_3O_{12}$	
B4	659	0.52
B4	704	0.14
B8H	659	0.50

[a] The rate of butadiene formation, v, was fit to $v \propto (p_{O_2})^n$, where p_{O_2} is the oxygen partial pressure.

whether the differential rates of butadiene formation over MoO_3 activated Bi_2MoO_6 depend on oxygen partial pressure. Interestingly, there appears a half-order ($\frac{1}{2}$) in oxygen partial pressure dependency at 659 K which decreases to approximately $\frac{1}{6}$ order at 704 K. Further investigation with $Bi_2Mo_3O_{12}$ catalysts yielded similar results, as shown in Table 3. Since we could not find a butadiene inhibition for the α phase catalysts, there is some justification for accepting a half-order oxygen dependency below 673 K at oxygen partial pressures far below 1700 Nm^{-2} for all selective γ phase catalysts. Experiments that will be discussed in the following were hence restricted to concentration ranges 1 C_4H_8 : 1 O_2 : 4 He and 10^5 Nm^{-2} (780 torr) total pressure.

In these studies, a number of experiments ("runs") at C_4H_8/O_2 ratio of about one were designed to evaluate the influence of contact time, t_c, at various temperatures. Contact time, t_c, was based on the reactor volume packed with catalyst divided by the total actual feed flowrate. The standard flowrate, F_T, in sccm (standard cm^3/min), was referenced to 298 K and 760 torr. The majority

TABLE 4

Catalysts and Runs for Various Contact Times and Catalyst Charges (Ratios C_4/O of 1-Butene and Oxygen are Given as Molecules/Atoms)

No.	Run (26)	Catalyst	F_T, sccm	C_4/O	Catalyst/SiC*
a1	29-34	A7	143	14.9/30	0.41/1.69
a2	29-34	A7	143	13.6/29	id.
b	36-8	A11	262	14.4/29	0.40/1.40
c	63-5	A8	275	15.3/30.4	0.41/2.92
d	47-56	A7	321	14/22.8	0.40/2.95
e	47-56	id.	596	13.9/27	id.
f	47-56	id.	611	13.2/27	id.
g	47-56	id.	622	13.7/24	id.
k	47-56	id.	837	12/24	id.
m	70	A31	995	10.3/29	0.34/1.35

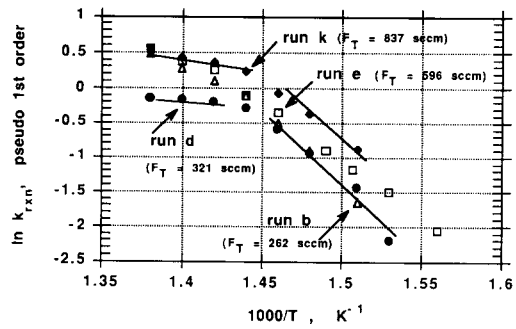

FIG. 7. Arrhenius plot of pseudo first-order rate constants versus $1/T$ for various Bi_2MoO_6 catalyst runs; feed conditions: 14% C_4H_8 : 13.5% O_2 : 72.5% He.

of the runs were performed on our base case γ-Bi_2MoO_6 catalysts but a few took place on base case α-$Bi_2Mo_3O_{12}$ catalysts.

Ten runs were performed on the γ catalysts; five were performed on the same catalyst charge, with F_T equal to 837, 622, 611, 596 and 321 sccm. Another five runs were performed on different catalyst charges but of similar constitution at F_T equal to 995, 275, and 262 sccm, and two runs at 143 sccm, I and II, as shown in Table 4. At a total feed flowrate of 143 sccm and a reaction temperature of 713 K, the contact time was one second. The contact times varied by about a factor of 10 for the flowrates and temperatures used. Figure 6 offers a representative collection out of the 10 runs: runs k, e, and d of Table 4 with F_T equal to 837, 596, and 321 sccm, respectively, with conversions to butadiene plotted as a function of temperature.

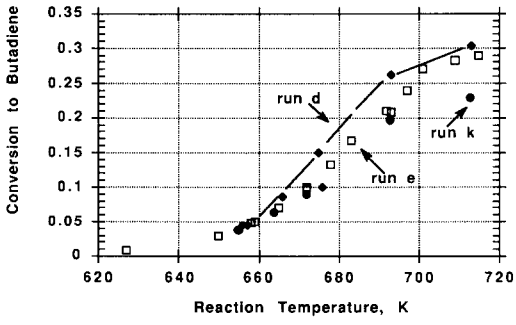

FIG. 6. Conversion to butadiene over Bi_2MoO_6 at various temperatures and total flowrates, F_T, at constant feed conditions: 14% C_4H_8 : 14% O_2 : 72% He.

The preliminary procedure used to formulate the kinetics assumed the rate of butadiene formation to be first order in butene partial pressure. The simplified expression for first order kinetics used was $kt_c = -\ln(1 - x)$, where x is the fractional conversion to butadiene, and k is the first order rate constant. To search for gross temperature dependence behavior, ln k was plotted versus $1000/T$ (where temperature, T, is in K). Since for first-order kinetics we might expect k to be equal to $k_1/(1 + K_D x)$, where K_D is an adsorption equilibrium reaction for butadiene, the plot would consist of two parts: at high T, K_D is small (inhibition-free) and $k = k_1$, whereas at low T, K_D is large (strong inhibition) and $k = k_1/K_D$. Four sets of data were selected and plotted in Fig. 7 out of ten as particularly illustrative; where the line drawn through the experimental data had a break (change of slope), the point will be named the break point. As an argument for the validity of the model, we refer to Fig. 3 in which two runs were compared that are similar in all respects except for the presence of butadiene in the feed. The run with butadiene in the feed shows the conversion of 1-butene to be shifted toward higher temperatures, thus showing that the break point position is determined by higher buta-

TABLE 5

Arrhenius Parameters of Catalytic Oxidation of 1-Butene to Butadiene over Bi_2MoO_6 + 4% Mo as a Function of Temperature and F_T

F_T, sccm	Rxn temperature > 673 K			Rxn temperature < 673 K		
	$R^2(n)$	a	$-b$	$R^2(n)$	a	$-b$
995	0.99(6)	7.3	4.9		not enough data	
837	0.98(4)	6.5	4.3	0.98(4)	19.9	13.7
622	0.95(4)	8.6	6.0	0.94(4)	33.7	23.3
611	0.99(3)	7.1	4.8	0.99(4)	30.7	21.1
596	1.00(3)	7.4	5.0	0.99(6)	27.9	19.2
321	0.91(4)	6.0	4.1	0.99(4)	22.5	15.4
262	1.00(4)	13.3	9.7	1.00(3)	34.2	23.7
143	0.98(4)	9.9	7.2	0.98(4)	23.5	16.6
Averages (F_T > 500) →		7 ± 1	4.8 ± 0.5	Avg →	28 ± 5	19.4 ± 3.4
Averages (F_T < 500) →		10 ± 4	7 ± 4	Avg →	22 ± 7	16.7 ± 3.3

diene partial pressure, i.e., inhibition. It was also found that by increasing F_T, thereby decreasing butene conversion, the break point was again moved towards lower temperatures. For instance, in run m (Table 4, F_T = 995 sccm) the break point was observed at 673 K, while in run d (Table 4, F_T = 321) the break point was observed at 703 K. The kinetics therefore appeared relatively simple: above the break point temperature, the noninhibited reaction dominates and below this the inhibited reaction does. Actually, the situation is more complicated since the oxygen partial pressure influences the rate of butadiene formation, as shown in Table 3 and Figure 5. This complication is dealt with later in the discussion, where it is accounted for. The kinetic data calculated for butadiene formation and the averages over the various runs are given in Table 5 (linear least squares was used for all fits). Runs with short contact times (typically F_T > 500 sccm) approaching differential conditions presented special opportunities for studying the reaction relatively free from inhibition at temperatures above 673 K. The number of data points that were covered by the straight line over a given temperature range were counted (e.g., 6 for F_T = 995 but only 4 for F_T = 321) and defined as their weights and mentioned in brackets as $R^2(n)$, as shown in Fig. 5. For the weighting procedure, rate constants were plotted as $\ln k = a - 1000b/T$ and the temperature range over which a straight line was fit, the weighted average of parameters a and b, given in Table 5, were calculated. Consider set of five F_T values, 995–596, in Tables 4 and 5 at temperatures above 673 K. The five a and b values appeared sufficiently near to each other to justify averaging. The rate parameters obtained were $a = 7.4 \pm 0.7$ and $b = -4.8 \pm 0.5$, while at 723 K the $\ln k$ value was +0.73, or $k = 2.0\ \text{sec}^{-1}$. The Arrhenius parameters of this catalytic reaction then became $\ln A = 7.4$ and $E_a = 40$ kJ/mol (9.5 kcal/mol). The final rate parameters for the

TABLE 6

Bi^{3+}/MoO^{6+} Ratios and Cation $\square^+$ and Anion $\square^-$ Vacancy Densities

Species	Proposed structural arrangement				Bi/Mo ratio
Bi_2O_3	Bi_{18}^{3+}	$\square_9^-$		O_{27}^{2-}	∝
γ-Bi_2MoO_6	Bi_{12}^{3+}		Mo_6^{6+}	O_{36}^{2-}	2
	Bi_{10}^{3+}	$\square_1^+$	Mo_7^{6+}	O_{36}^{2-}	1.43
	Bi_9^{3+}	$\square_{1.5}^+$	$Mo_{7.5}^{6+}$	O_{36}^{2-}	1.20
β-$Bi_2Mo_2O_9$	Bi_8^{3+}	$\square_2^+$	Mo_8^{6+}	O_{36}^{2-}	1.00
α-$Bi_2Mo_3O_{12}$	Bi_6^{3+}	$\square_3^+$	Mo_9^{6+}	O_{36}^{2-}	0.67
MoO_3		$\square_6^+$	Mo_{12}^{6+}	O_{36}^{2-}	0.00

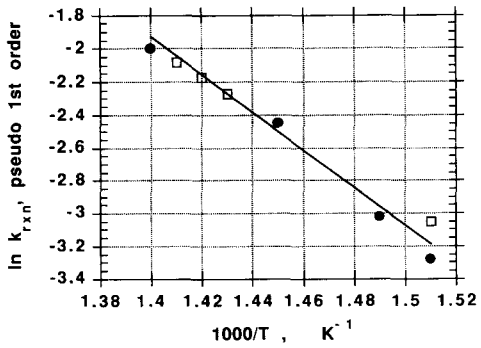

FIG. 8. Arrhenius pseudo first-order plot for $Bi_2Mo_3O_{12}$ versus $1/T$ for two catalyst runs; feed conditions: 14% C_4H_8: 13.5% O_2: 72.5% He.

inhibited reaction ($T < 673$ K) at the short contact times were $a = 28.0 \pm 4.8$ and $b = -19.4 \pm 3.4$, and although helpful, need further analysis before being acceptable as significant.

Results of experiments over $Bi_2Mo_3O_{12}$ were more difficult to analyze because we found the catalyst to be at least a factor of 12 less active on a mass basis; note that there was hardly any formation of CO_2 for these catalysts. Two runs at F_T equal to 995 and 260 sccm were used and after normalizing for contact time were found to give nearly identical results; see Fig. 8. No break point could be observed in the ln k vs $1000/T$ plot, in good agreement with the observation reported above that no butadiene inhibition could be found for this catalyst. The single line that represents the two runs has the parameters $\ln k = 13.5 - 11.1 \times 1000/T$.

DISCUSSION

Let us first summarize the various sets of Arrhenius pairs of constants obtained so far under the constraint that they belong to runs performed at high throughputs ($F_T > 500$ sccm) and temperatures above the break point; the runs are therefore free from inhibition by butadiene. They are for Bi_2MoO_6 + 4% MoO_3, $\ln A = 7.4$, and $E_a = 40$ kJ/mol and for base case $Bi_2Mo_3O_{12}$, $\ln A = 13.5$, and $E_a = 93$ kJ/mol. It is necessary to emphasize that the pure γ phase is an inferior catalyst; its activity is low and its selectivity is poor, in agreement with Matsuura *et al.* (*13*). If in the following the catalytic properties of the γ phase are discussed, we are referring to the "activated" species, Bi_2MoO_6 + 4% MoO_3 with a surface Bi/Mo ratio of 1.5 and a high activity; it shall be named γ^*. Let $Y(\gamma)$ denote the nonselective mode and X the selective oxidation mode for γ^* catalysts; characteristic of either mode is diffusion of O^{2-} from the so called "oxygen inlet site" to the "reaction site" and inhibition by butadiene at temperatures below 673 K. Adding more MoO_3 leaves the catalyst approximately constant in activity down to a surface ratio Bi/Mo = 1. From that point on the activity decreases and in parallel the diffusion of O^{2-} through the bulk, the butadiene inhibition, and the $Y(\gamma)$ mode vanish gradually. For the α phase there is no X mode, no inhibition by butadiene, and, if any, only small bulk diffusion of O^{2-}; only the selective $Y(\alpha)$ mode remains observable. The activity is then decreased by a factor of 12; the surface area is a factor of 3 smaller, hence the activity per unit surface is four times lower.

Let us analyze the kinetics of butadiene inhibition more closely. The method proposed was to calculate two reaction constants k_1 and K_D, the former representing the absence of inhibition as found independently by extrapolation to temperatures above the break point. The rate expression, v, for butadiene formation, $v = k_1 C_{Bo}(1 - x)/(1 + K_D C_{Bo} x)$, was integrated to give the expression $[\ln(1 - x) + K_D\{x + \ln(1 - x)\}] = -k_1 t_c$, where C_{Bo} is the feed 1-butene concentration. The values for K_D were calculated, using k_1 independently found, from x versus t_c data and results plotted as ln K_D versus $1000/T$ to estimate Q, the heat of butadiene desorption enthalpy. This estimate gave a value of $Q = -375$ kJ/mol, where R^2, the square of the correlation coefficient, was equal to 0.97. This result seems incompatible with the low-temperature adsorption results of Matsuura *et al.* (*14–16*),

even for his strong adsorption of butadiene where the heat of adsorption was on the order of 85 kJ/mol. We speculate that our data belong to an adsorption of butadiene with concomitant oligomerization ("polymerization") in the pores of the catalyst. A consequence of this hypothesis is that part of the oxidation occurs in these pores once the polybutadiene has been desorbed above 673 K. Provided the pore diameters are on the order of a few nm, the selective *X* reaction might hence occur predominantly in the pores. Before proceeding with this idea, let us first specify two mechanisms; first for the selective reaction (a somewhat modified Burrington–Grasselli model), and second for the gas phase unselective reaction initiated at the surface (in essence the Keulks model (*3*)).

All Surface Model

$$C_4H_8 + \underline{Mo^{6+}} + \underline{Bi^{3+}O^{2-}} \rightarrow \underline{Bi^{3+}OH^-} + \underline{Mo^{5+}[C_4H_7]^*} \quad (1)$$

$$\underline{Mo^{5+}[C_4H_7]^*} + \underline{Bi^{3+}O^{2-}} \rightarrow \underline{Bi^{3+}OH^-} + \underline{Mo^{4+}} + C_4H_6 \quad (2)$$

$$2\underline{Bi^{3+}OH^-} \rightarrow \underline{Bi^{3+}O^{2-}} + \underline{Bi^{3+}\square^a} + H_2O \quad (3)$$

$$\underline{Mo^{4+}} + \underline{Bi^{3+}} \rightarrow \underline{Mo^{6+}} + \underline{Bi^{1+}} \quad (4)$$

$$O_2 + 2\underline{Bi^{1+}} + 2\underline{\square^a} \rightarrow 2\underline{Bi^{3+}O^{2-}} \quad (5)$$

The symbol $\square^a$ means an empty oxygen atom site; an underline means on the surface, no underline means in the gas phase, and * means radical.

During reactions (1) and (2), two protons are donated from 1-butene to basic oxygen anions connected to two Bi^{3+} cations while two electrons are donated to Mo^{6+} and butadiene is released into the gas phase. In reaction (3), H_2O is liberated and an anion vacancy connected to Bi^{3+} is formed. Reaction (4) is an electron transport through the solid from Mo^{4+} to Bi^{3+} and in the final reaction, (5), two Bi^{1+} cations are oxidized by an oxygen molecule and the oxygen anions placed at the anion vacancies formed in reaction (3). Molecular species underlined occur on the surface. It should be noted that the redox reaction (4) could also be formulated with the help of the $Bi^{3+} \leftrightarrow Bi^{5+}$ electron exchange as is commonly accepted for the $FeSbO_4$ catalyst. The reaction sequence would then start at reaction (3).

Surface Initiated Homogeneous Gas Phase Reactions

These reactions are usually chain reactions, the chains being often branched. The chain carriers are atoms or radicals and are denoted as R*. Knowledge of the initiation and termination reactions of carriers on solid surfaces is minimal. Let us pattern the initiation reaction as similar to reaction (1):

$$C_4H_8 + \underline{Mo^{6+}} + \underline{Bi^{3+}O^{2-}} \rightarrow \underline{Bi^{3+}OH^-} + \underline{Mo^{5+}} + C_4H_7^* \quad (6)$$

Once the initiation reaction has been chosen the butadiene radical will react along a certain well-known pattern that finally leads to CO_2 and H_2O. Also electron transfer from Mo^{5+} to Bi^{3+} and further electron transfer to O_2 will take place as given in reactions (4) and (5). The only essential difference between the two mechanisms is that reaction (3), a second proton transfer, does not figure in the radical mechanism. We speculate that radicals in pores have a good chance to collide with another $Bi^{3+}O^{2-}$ surface group while radicals at an outer particle face may escape into the gas phase. In other words, reactions in narrow pores may be selective while reactions at outer surfaces run a good chance of developing into a combustion.

If the reaction network proposed in the all surface model is correct, the Bi/Mo ratio for maximum operation would be 1; the next question should be then what would be the structural elements of the best catalyst. Table 6 gives a survey of these elements for all structures between Bi_2O_3 and MoO_3. Note that Bi_2O_3 is represented as $Bi_2O_3\square^-$ which stands for a defect cubic eightfold oxygen surrounding with one of every four O^{2-} missing, and, hence, an oxygen vacancy

$\square^-$. Addition of Mo^{6+} leads to an idealized Bi_2MoO_6 structure with neither anion nor cation vacancies. According to the reaction network it should be inactive as indeed it is. If we start exchanging $2Bi^{3+}$ with $Mo^{6+} + \square^+$, that is, if we activate the γ structure by adding MoO_3, all elements for an active catalyst are present although as yet not at maximum activity; this is only reached when Bi/Mo = 1. Proceeding still further by replacing $2Bi^{3+}$ by $Mo^{6+} + \square^+$, the activity decreases again because it is dictated by the cation with the lowest concentration. Consistency demands that MoO_3 be inactive which is almost correct.

Moreover, β-$Bi_2Mo_2O_9$ should have maximal activity and γ^* and α about half that activity. Although this model is qualitatively attractive it needs some corrections before being quantitatively significant. The point to discuss in this connection is the differences between the selective butene oxidation over γ^*-Bi_2MoO_6 and over α-$Bi_2Mo_3O_{12}$ while the product distributions are the same. For instance, we believe that the selective X mode reaction over γ^* occurs in pores, the same pores that adsorb butadiene while no adsorption of butadiene was observed over the α phase. This checks with the works of Van Oeffelen *et al.* (*19*) and Graves and Buker (*20*), who found massive reduction of the γ phase by 1-butene in the absence of O_2 that ultimately led to the formation of metallic Bi while a similar reduction localized at the surface gave no formation of Bi^0. Factors other than pore versus surface reaction must be important. Before entering this discussion we shall take a second look at the pore structure of γ-phase Bi_2MoO_6.

The macroscopic texture of the catalyst indicates that the catalyst consists of a loose stapling of particles with diameters on the order of microns; there should exist pores with similar dimensions. This pore structure is not relevant for our purposes because its surface area is a factor of 10^3 too low; there should be another system with smaller pores. We assume that this system is present in the primary particles with diameter between 0.3 and 0.5 mm. Bi_2MoO_6 has a density of 8 g/cm^3 (*13*); the number of particles per gram is then 10^3 with a total surface area of 1.5×10^{-3} m^2/g while the experimental surface area is 2.5 m^2/g. Almost the entire surface is therefore located in the particles. It is noteworthy that the surface area does not change much by the activation with MoO_3; the primary pores are therefore already present in pure Bi_2MoO_6, their concentration dependent on the calcination temperature. To make this quantitative we shall assume that the primary pores all run in a vertical direction with length, l, while there are n square pores with side of length d. The sum of volumes of all pores per particle V and the sum of their surfaces S will then be $V = nld^2$ and $S = 4ndl$. Here, $l = 5 \times 10^5$ nm and there are 10^3 particles per gram. Hence, S per g $= 2dn \times 10^9$ nm^2 = 2.5 m^2. For an estimate of V we use data of Matsuura *et al.* (*13*), where the density of bulk Bi/Mo = 1.85 catalyst was about 7 g/cm^3, which means that $\frac{1}{8}$ of the bulk volume is empty; so $nld^2 = l^3/8$. Consequently we find that $d = 24$ nm and $n = 5 \times 10^7$. The total surface area of the pores per gram checks with 2.5 m^2/g. There is one per 5×10^3 nm^2 and the distance between pores is 70 nm. The model appears internally consistent; it exhibits a surface area that is of the right order but still contains enough solid phase to be coherent. We tried to apply the same calculation for the α phase. The necessary information on the density was derived from Matsuura's paper again (*13*). The density per unit cell is 6.2 (g/cm^3); because of uncertainties in extrapolating we chose two values for the real densities, viz., 6.0 and 5.8. Our surface areas were 0.72 m^2/g and the primary particle size was 0.32 mm. For the densities of 6 and 5.8 we find d to be 29 and 58 nm, respectively, with n values of 4 and 2×10^6, respectively. Consequently, the pore sizes for both catalysts, α-$Bi_2Mo_3O_{12}$ and γ^*, appear similar, the latter having fewer pores per mass.

Hence, according to theories for pore diffusion (see Weisz, for example, (*28*)), the

corresponding diffusivities for pore sizes of the order 25 nm should not cause significant mass transport resistances (*25*), and the hypothesis of the inhibition effect from butadiene to account for the loss in activation energy for γ^* catalysts seems plausible. This hypothesis is also supported by results given in Part I (see (*25*)): the diffusivities for butene (and butadiene) were estimated to be on the order 0.1 cm^2/sec and it was also shown by calculation and experiment that both external and internal mass transfer resistances were largely absent. In addition, coke formation by butadiene was also ruled out as a possible alternative explanation for the loss in activation energy for γ^* catalysts since it was experimentally observed that butadiene inhibition was entirely reversible: on the time scale of GC sampling time (10–30 min), it was possible to go back and forth from the two curves in Fig. 3. Oxidatively burning off coke from the catalyst would be a slower, diffusion-limited process (compared to diene desorption) and would potentially display more significant time lags in butene conversion and catalyst temperatures (exotherms), neither of which were experimentally observed.

The next question is why $Y(\alpha)$ is selective and not $Y(\gamma)$. The difference between the two cases should be caused by the difference of their Bi/Mo ratios. For the selective catalyst the ratio $Bi/Mo/\square^a = 2:3:1$ and for the nonselective catalyst 10 : 7 : 1. Since butene enters the reaction via the Mo^{6+} and $Bi^{3+}O^{2-}$ pair and O_2 via Bi^0 and excess Bi^{3+} at the outer surface might lead to an increases tendency for oxidizing the nascent $C_4H_7^*$ radical. It might be speculated that the excess of Bi might lead to formation of $Bi^{5+}O_2^{-2}$ causing peroxy radical formation and combustion at the surface. Such an effect would not be feasible for the Bi-poor centers of the α phase. This effect might hence be explainable as another example of the influence of the *ensemble composition* in heterogeneous oxidation (see Straguzzi (*29*)).

It is possible to explain in terms of the following proposed catalytic cycle, incorporating the Keulks–Krenzke ideas for oxygen diffusion and consistent with the all surface model, how the oxygen partial pressure dependence figures into the kinetic expression. Reactions (1) through (5) are restated as follows:

Catalytic Cycle with Ensembles E_1 and E_2

$$B + E_1 \leftrightarrow B''E_1H \quad (7)$$

$$B''E_1H \rightarrow E_1R + D + H_2O \quad (8)$$

$$D + E_1 \leftrightarrow DE_1 \quad (9)$$

$$E_2 + E_1R \leftrightarrow E_2R + E_1 \quad (10)$$

$$O_2 + 2E_2R \leftrightarrow 2E_2 \quad (11)$$

where B means 1-butene (B″ for adsorbed), D means butadiene, E_1 represents the ensemble of one Mo and two Bi moieties responsible in Eqs. (1) and (2) above for the abstraction of two protons, and E_1R represents the $Bi^{1+}\square$ reduced moiety. Now, it is proposed that an equilibrium exists between the surface ensembles E_1 and E_2, Eqs. (10) and (11), in which oxygen dissociates onto reduced E_2R. One rate expression found (*26*) for butadiene formation which fit the observed kinetic behavior over γ^*-Bi_2MoO_6 catalysts was derived assuming reaction (8) to be irreversible, with rate constant k_8, and with all other steps at equilibrium, with respective equilibrium constants, K_i, for the ith equation. For this case, the rate expression, v, is $v = k_8[B''E_1H] = k_8K_7[B][E_1]$. The total ensemble balance, L_1, for ensemble E_1 is $[L_1] = [E_1] + [DE_1] + [E_1R] + [B''E_1H]$. The rate expression, after simplification, is given by $v = k_8[L_1]K_7[B][O_2]^{1/2}KS/\{1 + KS[O_2]^{1/2}(1 + K_9[D] + K_7[B])\}$, where $KS = K_{10}(K_{11})^{1/2}$. At high temperature and differential conditions (i.e. $[D] = 0$ and $[O_2] =$ constant), $[L_1] = [E_1]$ and $v = k_8[L_1][B]$; i.e. pseudo-first order kinetics. At low temperature and initial conditions ($[D] = 0$), $[L_1] = [E_1R]$, and $v = k_8[L_1][B]KS[O_2]^{1/2}$, as observed for all γ^* type catalysts. At low temperature and high butadiene partial pressure, $[L_1] = [DE_1]$, and v, in the limit

of sufficiently high [D], tends to zero due to complete inhibition. *Prior to complete inhibition,* we see that the denominator in rate v is dominated by $KS[O_2]^{1/2}(1 + K_9[D])$, so that the half order dependence of oxygen partial pressure mathematically cancels and would not be observed experimentally. Furthermore, the cancellation of oxygen partial pressure dependence gives support to the calculation presented earlier for the heat of diene adsorption, $-Q$, since, in this limit, $v = k_8[L_1]K_7[B]/(1 + K_9[D])$, and this was precisely the expression used in the Q calculation. At high temperature, the bulk solid phase equilibrium of oxygen atoms is hypothesized to be fast, so that the term K_{10} gets large, tending to a zero order oxygen dependence, as semiquantitatively observed. Hence, it can be seen that rate v agrees with the observed kinetic behavior and moreover supports the argument of polybutadiene formation and large Q.

For the α type catalysts, a similar rate expression was derived; however, the ensembles for this catalyst, E_3 and E_4, are perhaps different, especially with respect to butadiene adsorption characteristics. The ensemble balance for ensemble E_3 is $[L_3] = [E_3] + [E_3R] + [B''E_3H]$. The rate expression, v' (note the primes, ('), used), after simplification, is

$$v' = k_{8'}[L_3]K_{7'}[B][O_2]^{1/2}KS'/\{1 + KS'[O_2]^{1/2}(1 + K_{7'}[B])\}.$$

We see that expressions v and v' are identical in form except for the missing butadiene inhibition term in v'. Intriguing is the unique O_2 dependence observed both experimentally and predicted by both rate expressions. The O_2 partial pressure dependence decreases with increasing temperature. This trend is opposite to what one expects for typical catalysts wherein only surface species are involved in the catalytic cycle, Langmuir–Hinshelwood (LH) type kinetics. In LH type kinetics, it would be expected that the O_2 partial pressure order should increase as the temperature increases since the number of adsorbed surface oxygens decreases as the temperature increases (bare surface sites are filled with dissociated oxygen at lower temperatures). However, the unique behavior common for the bismuth molybdate catalysts is apparently due to the dynamic equilibrium between active surface and lattice oxygen atoms, expressed in rates v and v' above as a dynamic surface ensemble 1 ↔ bulk catalyst ↔ surface ensemble 2 equilibrium established at steady state between the oxygen inlet and oxygen outlet locations of this bifunctional catalyst. The terms KS and KS' apparently increase with temperature (faster equilibrium), in line with observed kinetics.

When summarizing our results we conclude that most of the new insights concerning the butadiene kinetics, especially the role of oxygen and butadiene inhibition, were only possible with isothermal continuous flow laboratory reactors and careful analytical studies. Selectivity and activity differences in Bi molybdates were explained in terms of the catalysts' surface composition, an example of the *ensemble effect* in heterogeneous oxidation.

ACKNOWLEDGMENTS

The authors thank Drs. J. A. Onuferko and P. Dismore for their valuable discussions and technical assistance on surface and bulk characterization of the catalysts, respectively, and acknowledge the technical assistance of Dr. K. Dooley and the analytical group at DuPont. We thank the Center for Catalytic Science and Technology at the University of Delaware for financial support. This work formed the subject of part of a Ph.D. Thesis, University of Delaware, Department of Chemical Engineering, Center for Catalytic Science and Technology.

REFERENCES

1. Gates, B. C., Katzer, J. R., and Schuit, G. C. A., "Chemistry of Catalytic Processes," Chapter 4, McGraw-Hill, New York, 1979.
2. Hucknall, D. J., "Selective Oxidation of Hydrocarbons," Academic Press, New York, 1974.
3. Keulks, G. W., *Adv. Catal.* **27,** 183 (1978).
4. Schuit, G. C. A., *J. Less-Common Met.* **36,** 329 (1974).
5. Sachtler, W. M. H., and De Boer, N. H., *in* "Proceedings of the International Congress on Catalysis, 3rd, Amsterdam, 1964" (W. M. H. Sachtler,

G. C. A. Schuit, and P. Zweitering, Eds.), Vol. 1, p. 252, North-Holland, Amsterdam, 1965.
6. Mars, P., and Van Krevelen, D. W., *Chem. Eng. Sci. Suppl.* **33,** 420 (1954).
7. Keizer, K., Batist, P. H., and Schuit, G. C. A., *J. Catal.* **15,** 256 (1969).
8. Prette, H. J., Batist, P. H., and Schuit, G. C. A., *J. Catal.* **15,** 267 (1969).
9. Elzen, Van Den, A. F., and Rieck, G. D., *Acta Crystallogr. Sect. B* **29,** 2433 (1973).
10. Elzen, Van Den, A. F., and Rieck, G. D., *Mater. Res. Bull.* **10,** 1163 (1975).
11. Buttrey, D. J., Jefferson, D. A., and Thomas, J. M., *Mater. Res. Bull.* **21,** 739 (1986).
12. Batist, Ph. A., Der Kinderen, A. H. W. M., Metz, F. A. M. G., Leeuwenburgh, Y., and Schuit, G. C. A., *J. Catal.* **12,** 45 (1968).
13. Matsuura, I., Schut, R., Hirakawa, K., *J. Catal.* **63,** 152 (1980).
14. Matsuura, I., *J. Catal.* **33,** 420 (1974).
15. Matsuura, I., and Schuit, G. C. A., *J. Catal.* **20,** 19 (1971).
16. Matsuura, I., and Schuit, G. C. A., *J. Catal.* **25,** 314 (1972).
17. Keulks, G. W., *J. Catal.* **19,** 232 (1970).
18. Keulks, G. W., and Krenzke, L. D., *in* "Proceedings of the International Congress on Catalysis, 6th, Imperial College, London, 1976" (Geoffrey C. Bond, Peter B. Wells, and F. C. Tompkins, Eds.), preprint B-20, Royal Soc. Chem., London, 1977.
19. Van Oeffelen, D. A. G., Van Hooff, J. H. C., and Schuit, G. C. A., *J. Catal.* **95,** 84 (1985).
20. Graves, C., and Buker, R. A., *J. Catal.* **108,** 247 (1987).
21. Burrington, J. D., and Grasselli, R. K., *J. Catal.* **59,** 79 (1979).
22. Burrington, J. D., Kartisek, C. T., and Grasselli, R. K., *J. Catal.* **87,** 363 (1984).
23. Anderson, A. B., Ewing, D. W., Kim, Y., Burrington, J. D., Burrington, J. D., and Grasselli, R. K., *J. Catal.* **96,** 222 (1985).
24. Haber, J., Sochacka, M., Grzybowska, B., Golzbiewski, A., *J. Mol. Catal.* **1,** 35 (1975).
25. Burban, P. M., Schuit, G. C. A., Koch, T. A., and Bischoff, K. B., *J. Catal.*, **126,** 317 (1990).
26. Burban, P. M., Ph.D. Thesis, University of Delaware, Department of Chemical Engineering, Center for Catalytic Science and Technology, 1984.
27. Schuit, G. C. A., Personal communication, Jan. 1981.
28. Weisz, P. B., *Chem. Technol.*, 504 (1973).
29. Straguzzi, G., Ph.D. Thesis, University of Delaware, Department of Chemical Engineering, Center for Catalytic Science and Technology, 1985.